The formation of fibrolite nodules in a package of melanocratic gneisses from the Hercynian basement of NE Sardinia, Italy.

by *Marcello Franceschelli*[1], *Fortunata Pannuti*[1] and *Gianfranco Carcangiu*[2]

Abstract

The formation of fibrolite nodules in melanocratic gneisses on the margins of an orthogneiss from NE Sardinia was examined.

The length and the width of the nodules range from 0.2 to 4 cm and from 0.1 to 1 cm respectively. Quartz, fibrolite and biotite are the major minerals (total volume percent in the range 95–99%).

The model proposed for the formation of fibrolite nodules involves two distinct processes:

– the formation of fibrolite in dominantly lens-shaped-segregations, at the peak of Hercynian metamorphism, parallel to and/or at small angles to S_1 foliation. The bulk of the fibrolite appears to be formed by the decomposition of S_1 biotite induced by the action of hydrogen ions.

– the transformation of lens-shaped fibrolitic segregations to nodules by tectonic deformation. During the late tectonic-metamorphic evolutionary stage of the Hercynian orogeny the fibrolite nodules underwent a muscovitization process.

Keywords: Fibrolite nodules, melanocratic gneiss, structural history, Sardinia, Hercynian orogeny.

Introduction

The fibrolite-bearing segregations have been described from many localities and in a great variety of host rocks including: medium and high grade pelitic schists, pelitic hornefels, porphyritic quartz monzonite and granitic pegmatite. An exhaustive review of the occurrence of the fibrolite and more in general of the Al_2SiO_5 segregations have been recently given by VERNON (1987) and KERRICK (1990 and bibliography therein).

Most of the models proposed for the formation of fibrolite segregations in the form of ovoidal nodules assumed the contemporaneous formation of nodules and fibrolite (LOSERT, 1968). On the contrary fibrolite and nodules may be produced by two distinct processes at different times, i.e. an Al_2SiO_5 producing reaction followed by a late deformation during the last evolutionary stage etc.

For a genetic model it is important to decipher the relationship between the formation processes of fibrolite and nodules.

This paper describes the fibrolite nodules formed in a package of melanocratic gneisses sourrounding an orthogneiss from the Hercynian basement of NE Sardinia. We discuss the fibrolite-forming reaction and present data supporting the idea that the nodules are the result of the folding and transposition of lens-shaped fibrolitic segregations formed by a base leaching process during the Hercynian amphibolite facies metamorphism.

Geological setting

The metamorphic geology of the NE Sardinian basement has been described by FRANCESCHELLI et al. (1982 a, b, 1989) and ELTER et al. (1986).

The metamorphic basement consists of a suite of multideformed phyllites, micaschists, gneisses, migmatites and igneous derived rocks such as augen gneisses, orthogneisses and amphibolites, which underwent prograde metamorphism during the Hercynian orogeny. The migmatitic rocks in-

[1] Istituto di Giacimenti Minerari, Geofisica e Scienze Geologiche, Piazza d'Armi, University of Cagliari, I-09100 Cagliari, Italy.

[2] Centro di Studi Geominerari e Mineralurgici C.N.R., Piazza d'Armi, I-09100 Cagliari, Italy.

PUNTA AINU

FIBROLITE NODULES

ORTHOGNEISS

MELANOCRATIC
GNEISSES

SEDIMENTS

10 m

N

S₂ SCHISTOSITY

D₂ FOLD AXES

FIG.1b

LEGEND

SEDIMENTS

HERCYNIAN GRANITOIDS

MICASCHISTS,
PARAGNEISSES AND
QUARTZITES

MIGMATITES, GNEISSES
AND ECLOGITES

AUGEN GNEISSES

GRANODIORITE
ORTHOGNEISS

BOUNDARIES OF
METAMORPHIC ZONES

LOCALITY

TYRRENIAN SEA

San Teodoro

Punta Ainu

SARDINIA

1 KM

FIG.1a

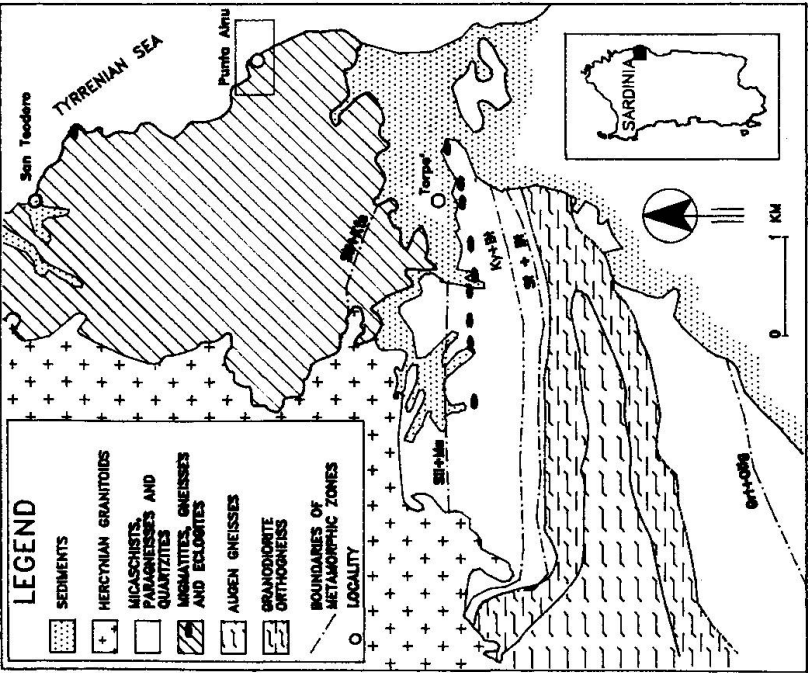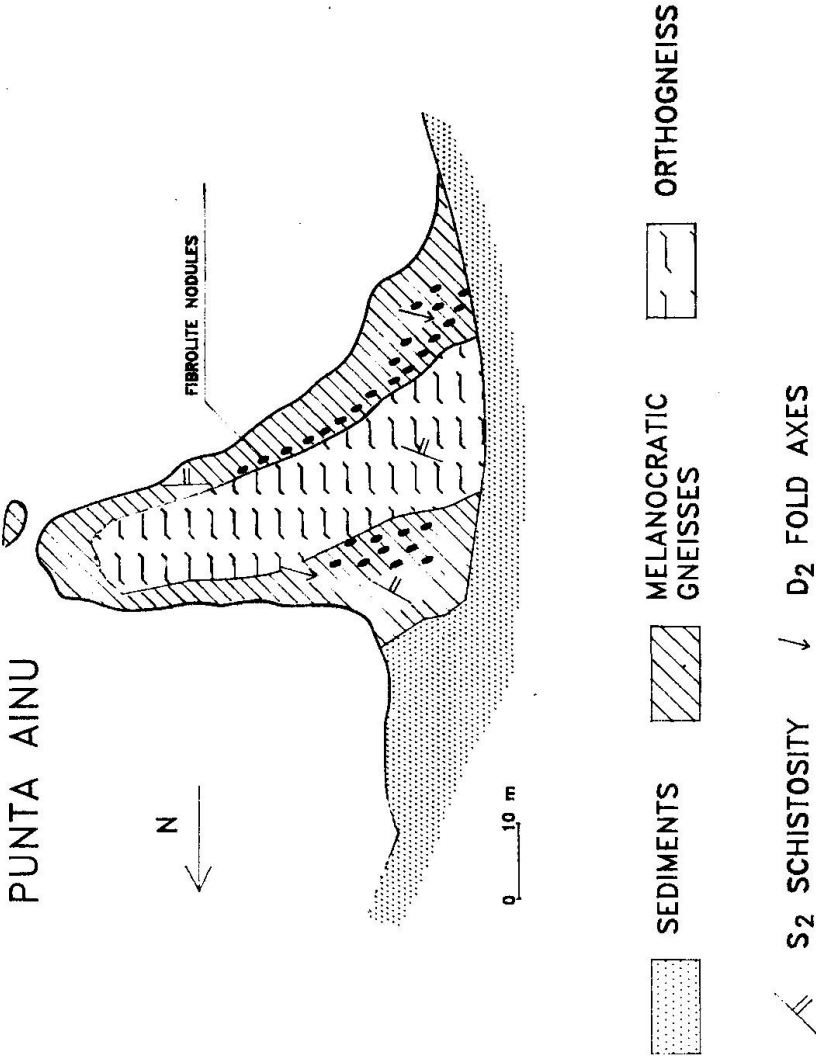*Fig. 1* a) Sketch map showing the metamorphic zonation of a portion of the basement of North East Sardinia. b) Map showing the main rock units in the Punta Ainu area and the relations between the occurrence of fibrolite nodules, orthogneisses and melanocratic gneisses. Some localities quoted in the text are also shown. Mineral abbreviations are according to KRETZ (1983); except: Olig = oligoclase; Fib = fibrolite.

clude metabasites with pre-Hercynian relics of granulite and eclogite facies assemblages.

The metamorphic grade increases from south to north perpendicularly to the general strike of the Hercynian belt. The following sequence of mineral zones (Fig. 1a): garnet, staurolite + biotite, kyanite + biotite, sillimanite + muscovite and K-feldspar + sillimanite has been mapped by FRANCESCHELLI et al. (1982b). The peak of metamorphism took place at about 344 ± 7 Ma and the basement uplift at about 310–300 Ma (FERRARA et al., 1978).

Punta Ainu is situated in the central part of the K-feldspar + sillimanite zone (Fig. 1a). The rocks outcropping at Punta Ainu (Fig. 1b) are orthogneisses surrounded by a 20–50 m thick package of melanocratic gneisses.

The metasedimentary rocks are of unknown age. The granodioritic orthogneiss of the garnet zone (Fig. 1a) yielded a Rb–Sr age of 458 ± 31 Ma, interpreted as the age of emplacement of the magmatic body (FERRARA et al., 1978).

The orthogneiss consists of K-feldspar, plagioclase, biotite and minor muscovite and garnet. The modal proportion of these minerals suggests a granitic composition.

The melanocratic gneisses contain calc-silicate nodules and minor migmatite, mostly of the stromatic type.

As shown in figure 1b the fibrolite nodules are hosted by the melanocratic gneisses near and along the contact with the orthogneiss. The fibrolite nodules are typically hosted by strong foliated biotite-rich gneisses and are lacking or scarcely present in the massive gneisses (Fig. 2). The fibrolite nodules are associated to pervasive quartz veins.

Structural history

On the high grade rocks of the Punta Ainu area three systems of small scale structures (D_1, D_2, D_3) followed by local shearing deformation can be recognized.

In spite of the good preservation of S_1 schistosity, no clear examples of D_1 folds are observed in the field.

Small scale D_2 folds affecting the migmatite

a)

b)

c)
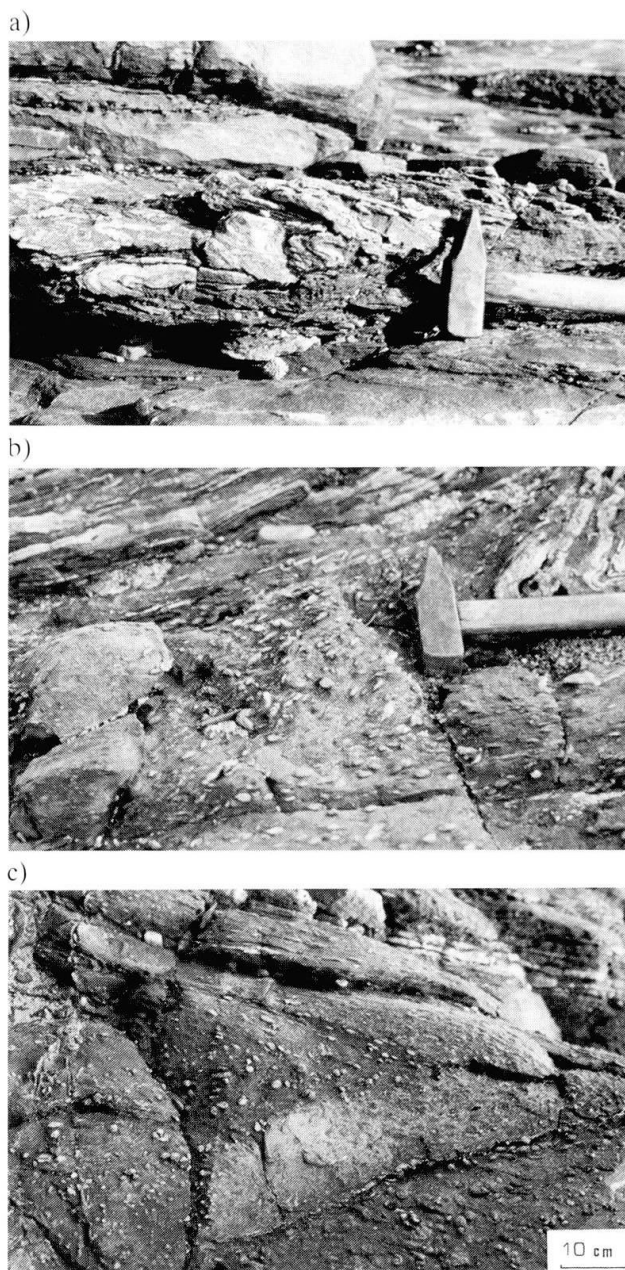
Fig. 3 Field photography of the D_2 folds in the melanocratic gneisses from Punta Ainu: a) intrafoliar nodule-free D_2 folds in the melanocratic gneisses. Note an early schistosity (S_1) below the hammer in the right side of the photo; b) quartz veins and fibrolite nodules; c) alternating nodule-rich and nodule-poor levels of melanocratic gneisses. S_2 schistosity is horizontal in the photo.

Fig. 2 Field photography showing the occurrence of fibrolite nodules in the foliated layers and their absence or rarity in the massive layers of the melanocratic gneisses.

Fig. 4 Sample photography showing the occurrence of fibrolite nodules in melanocratic gneisses perpendicular to the elongation of the nodules and perpendicular to the S2 schistosity, horizontal in the photo. N = fibrolite nodules. (See text for explanation.)

and melanocratic gneisses are the dominant field structure. The style of the D2 folds in the melanocratic gneisses is shown in figures 3 a, b, c. Their wavelengths are between 1–50 cm and their axes strike N 120–130° and dip southwards. The related S2 schistosity is pervasive and associated with extensive mineral growth.

The D3 folding phase in the Punta Ainu area is moderately weak and is associated with open folds of variable wavelengths. D3 fold axes strike N 130–140° and dip southwards (40–50°). S3 is a spaced axial plane schistosity which strikes N 055° and dips southwards; it is associated with relatively scarce mineral growth.

Locally the rocks of Punta Ainu show a weak mylonitic schistosity, overprinting the D3 folds. This deformation may be correlated with the mylonitic deformation affecting the medium grade rocks immediately south of this area (ELTER, 1986). Furthermore, it has produced cracking and fractures on the pre-existing minerals and growth of phyllosilicates.

The relationships between fibrolite nodules and the D2 folding phase are shown in figures 3 b, c and 4. In the limb region of the D2 fold the long axes of the nodules form a small angle with the S1 schistosity, while in the hinge region they are clearly folded (Fig. 4). On S2 the fibrolite nodules form an extensional lineation striking N 130–140°.

Petrography

THE FIBROLITE NODULES

The length and width of the nodules range from 0.2 to 4 cm and from 0.1 to 1 cm respectively. Typical fibrolite nodules are shown in figure 5. The nodules are wrapped around by the S2 schis-

tosity (Figs 5 a, b). Often the nodules are surrounded by a thin biotite rim or a biotite aureole (Fig. 4). They consist of fibrolite (30–70%), quartz (20–50%), biotite (10–20%) and minor plagioclase, garnet, sillimanite, kyanite, apatite, tourmaline and Fe-oxides. With the exception of
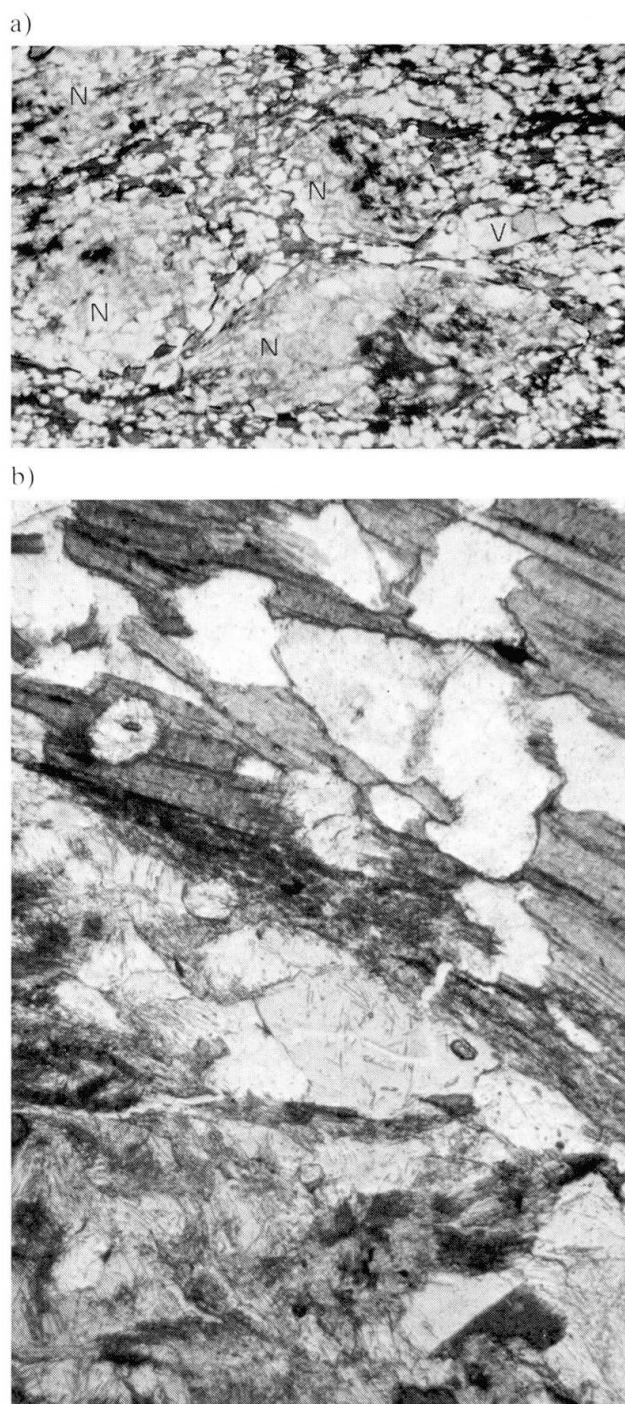
a)

b)

Fig. 5 Photomicrograph showing the relationships between the fibrolite nodules and S2 schistosity: a) nodules wrapped around by S2 schistosity. Width of photo corresponds to 5.2 mm; b) detail of a fibrolite nodule margin marked by the oriented biotite flakes of the host rocks. Width of photo corresponds to 1.3 mm. N = fibrolite nodules; V = quartz veins.

fibrolite, all the major and minor phases of the nodules also occur in the host rocks. Some large nodules display mineralogical zoning. They are made up of a core consisting of an aggregate of fibrolite needles and a border of fibrolite + biotite + quartz.

Fibrolite is often altered to fine grained white K-mica. The growth of muscovite is not pervasive. Nodules completely transformed to aggregates of muscovite and others unaffected by muscovitization can be observed in the same thin section.

THE MELANOCRATIC GNEISSES

The melanocratic gneisses consist of alternating strong foliated and massive to weakly foliated layers (Fig. 2). The strongly foliated layers are made up of biotite, plagioclase, quartz, garnet and small amounts of apatite and zircon. Tourmaline is a prominent accessory in rocks with abundant fibrolite nodules. The modal proportions of biotite range from 50 to 70 per cent. Sporadically entrapped crystals of kyanite and sillimanite are also observed in plagioclase crystals.

The mineralogy of the massive layers is identical to that of the foliated biotite-rich gneisses. Quartz and plagioclase are the dominant minerals while the biotite ranges from 5 to 10 per cent modal proportions.

Most of the samples studied do not contain muscovite. The muscovite usually occurs as medium to fine-grained flakes replacing biotite along the S_2 schistosity or near the margins of the mineral.

The melanocratic gneisses are very rich in quartz veins, about 0.5–5 cm thick and 10–80 cm long, which are more and more frequent as the fibrolite nodules increase. Plagioclase, fibrolite and biotite sometimes occur in the quartz veins.

Mineral chemistry

The mineral analyses were performed with an ARL-SMQ electron microprobe, operating in the wavelength dispersive mode at a 20 kW, 20 nA beam current and a 3–20 µm variable beam spot size. Natural microcline, ilmenite, olivine, anorthoclase, augite and lepidolite were used as standards. Raw data were corrected by the ZAF procedure, using the MAGIC IV program. Representative chemical compositions of fibrolite, sillimanite, kyanite, biotite, plagioclase, muscovite and tourmaline from four samples are given in table 1. Complete sets of analyses of other samples are available on request.
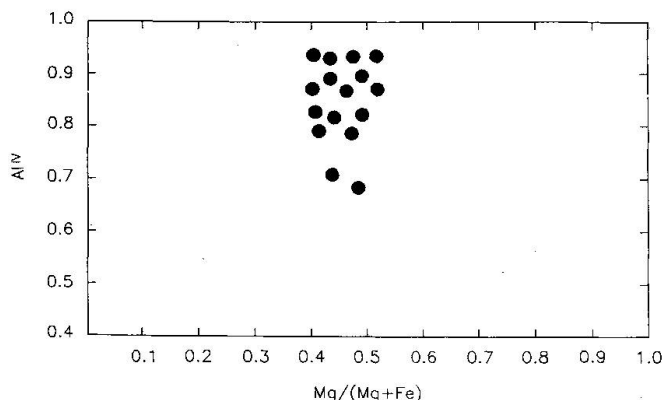

Fig. 6 Chemical composition of biotite in fibrolite nodules plotted in the Mg/(Mg + Fe) vs Al^{VI} diagram. Estimated relative average error of electron microprobe analysis 2%: Al; 3% Mg and Fe.

Al-silicates – The analyses of fibrolite, kyanite and sillimanite are reported in table 1. All three Al-silicates contain minor amounts of FeO < 0.24 (wt%) and trace amounts of MgO and MnO.

Plagioclase – Plagioclase crystals are usually unzoned. The anorthite content is close to An 21–25%. The maximum variation observed among the various crystals is 2–3% moles of anorthite. The K content is lower than 0.09 (a.f.u.). No compositional differences have been detected between the plagioclases of the host rocks and those of the nodules.

Biotite – The composition of biotite is illustrated in figure 6. The Mg/(Mg + Fe) ratio ranges from 0.40 to 0.51 with a cluster of values close to 0.45. The Al^{VI} ranges from 0.65 to 0.95. Ti is lower than 0.36 (a.f.u.), and Na lower than 0.08 (a.f.u.). The BaO and F contents are lower than 0.40 (wt%) and 0.16 (wt%) respectively. No systematic differences have been found between the composition of the fibrolitized biotite in the nodules and the S_2 biotite in the host rocks.

Garnet – Garnet is almandine-rich (65%) with a high spessartine content (19%) and a subordinate content of pyrope (13%) and grossularite (3%). The garnet enclosed in the plagioclase crystals is identical in composition to the garnet in the matrix. Both garnets are practically unzoned.

Muscovite – The Si content ranges from 6.05 to 6.18 (a.f.u.). The Mg/(Mg + Fe) ratio is close to 0.55. The K content ranges from 1.74 to 1.84 (a.f.u.) and the Na content from 0.08 to 0.12 (a.f.u.).

Other minerals analysed were apatite and tourmaline. The structural formula of tourmaline

Tab. 1   Representative electron microprobe mineral analyses from four specimens of melanocratic gneisses. Asterisk = fibrolite and retrograde muscovites in nodules. Structural formulae are calculated assuming all iron as ferrous iron. Mineral abbreviations as in KRETZ (1983).

SPECIMENS	S44					S40			
	Fib*	Ms*	Bt	Pl	Ap	Ky	Ms	Bt	Pl
SiO2	36.86	44.50	35.33	62.39	-	37.06	45.61	33.86	62.32
TIO2	-	0.09	2.20	0.02	0.02	0.03	0.10	3.15	-
Al2O3	61.84	32.62	19.55	23.08	-	62.59	35.54	18.65	22.97
FeO	0.24	3.01	18.15	0.05	0.29	0.15	0.81	19.31	-
MnO	0.03	0.10	0.20	-	0.45	0.01	0.03	0.20	-
MgO	0.03	2.15	9.22	0.02	0.06	-	0.56	9.76	-
CaO	-	0.06	0.04	4.36	54.12	-	0.04	0.02	4.36
Na2O	-	0.47	0.25	8.60	0.08	-	0.43	0.01	8.68
K2O	-	10.13	9.41	0.34	0.01	0.01	10.10	9.64	0.39
BaO	-	0.40	0.14	-	-	-	0.28	-	-
P2O5					41.68				
F	-	0.09	0.15	-	-	-	0.16	-	-
Total	99.00	93.62	94.73	98.86	96.71	99.85	93.66	94.65	98.72
	ions to 5 oxygens	ions to 22 oxy.	ions to 22 oxy.	ions to 8 oxy.	ions to 13 oxy.	ions to 5 oxy.	ions to 22 oxy.	ions to 22 oxy.	ions to 8 oxy.
Si	1.005	6.129	5.399	2.789	-	1.021	6.165	5.218	2.792
AlIV	-	1.871	2.601		-	-	1.835	2.782	-
AlVI	1.987	3.423	0.918	1.216		2.033	3.825	0.608	1.212
Ti	-	0.009	0.253	-	0.001	-	0.010	0.365	-
Fe	0.005	0.346	2.319	-	0.021	0.003	0.091	2.490	-
Mn	-	0.012	0.025	-	0.034	-	0.002	0.026	-
Mg	0.001	0.441	2.098	-	0.008	-	0.112	2.243	-
Ca	-	0.008	0.007	0.209	5.237	-	0.006	0.004	0.209
Na	-	0.125	0.074	0.756	0.014	-	0.112	0.002	0.753
K	-	1.779	1.834	0.019	0.001	-	1.741	1.897	0.022
Ba	-	0.022	0.008	-	-	-	0.015	-	-
F	-	0.038	0.073	-	-	-	0.067	-	-
P					3.071				
Mg/Mg+Fe	-	0.560	0.475			-	0.552	0.474	-

was calculated as outlined by HENRY and GUIDOTTI (1985). Tourmaline is Ca-poor with Na and K contents of 0.638 and 0.014 (a.f.u.) respectively. In the Al-Fe-Mg and Ca-Fe-Mg diagrams of HENRY and GUIDOTTI (1985), tourmaline plots in the typical field for tourmaline coexisting with an Al-saturated phase. Tourmaline is poorly zoned.

Formation of fibrolite nodules

Three main processes must be investigated in order to elaborate a genetic model for the fibrolite nodules: the fibrolite-forming reaction, the local process causing fibrolite clustering and the effects of subsequent tectonics.

Tab. 1 (continued)

SPECIMENS	S45				S35					
	Fib*	Ms*	Bt	Pl	Fib*	Sil	Bt	Pl	Tur	Grt
B_2O_3									10.65	
SiO_2	37.50	44.45	34.43	62.05	37.94	37.87	35.15	61.85	35.78	37.11
TiO_2	0.03	0.10	2.45	-	0.03	0.02	2.13	-	0.43	0.03
Al_2O_3	61.85	35.21	19.45	23.00	61.35	61.48	20.44	23.08	34.20	21.74
FeO	0.10	0.84	18.13	0.02	0.10	0.15	18.18	0.02	5.36	29.21
MnO	-	0.02	0.28	-	-	-	0.32	-	-	8.33
MgO	0.01	0.54	8.88	-	0.01	0.01	10.17	-	6.98	3.38
CaO	-	0.02	0.02	4.45	-	-	0.04	4.41	0.61	0.99
Na_2O	-	0.30	0.25	8.85	-	-	0.33	8.63	2.02	-
K_2O	-	10.46	10.03	0.31	-	-	9.36	0.53	0.09	-
BaO	-	0.63	-	-	-	:	0.40	-	0.06	-
F	-	0.06	0.15	-	-	-	0.12	-	-	-
Total	99.49	92.63	94.07	98.66	99.43		96.64	98.52	96.18	100.79

	ions to 5 oxygens	ions to 22 oxy.	ions to 22 oxy.	ions to 8 oxy.	ions to 5 oxy.	ions to 5 oxy.	ions to 22 oxy.	ions to 22 oxy.	ions to 29 oxy.	ions to 12 oxy.
B					-		-	-	2.997	
Si	1.016	6.110	5.326	2.784	1.028	1.026	5.269	2.781	5.837	2.963
AlIV	-	1.890	2.674		-		2.731		6.574	0.037
AlVI	1.975	3.813	0.817	1.216	1.959	1.962	0.879	1.223	-	2.008
Ti	-	0.010	0.285	-	-	-	0.239	-	0.053	0.002
Fe	0.002	0.096	2.345	-	0.002	0.003	2.278	-	0.731	1.950
Mn	-	0.002	0.036	-	-	-	0.041	-	-	0.563
Mg	-	0.111	2.047	-	-	-	2.271	-	1.696	0.402
Ca	-	0.003	0.003	0.214	-	-	0.006	0.212	0.107	0.085
Na	-	0.079	0.075	0.769	-	-	0.095	0.752	0.638	-
K	-	1.833	1.978	0.018	-	-	1.789	0.030	0.014	-
Ba	-	0.034	-	-	-	-	0.023	-	0.003	-
F	-	0.026	0.073	-	-	-	0.059	-	-	-
Mg/Mg+Fe	-	0.536	0.470		-	-	0.499	-	-	0.171

MINERALOGICAL EVIDENCE

The textures formed as grown fibrolite are illustrated in figures 7 a, b, c, d, e. When present in small amounts, fibrolite occurs as isolated needles growing on/and mantling the S_1 biotite flakes. At more advanced stages of biotite fibrolitization, fibrolite occurs as single needles (5 μm wide and 0.1 mm long), as acicular radiating aggregates or as pseudomorphic aggregates replacing biotite (Fig. 7a). The fibrolite occurs as needles oriented parallel to the cleavage of biotite (Fig. 7b) and forms the typical triangular arrangement within the basal plane as described by CHINNER (1961).

The acute angle between the oriented fibrolite needles was carefully measured with a universal stage. The measurement typically yielded a statistical concentration of values between 56 and 64 degree.

The end product of the biotite breakdown is a fibrolite aggregate in which only minute traces of biotite remain (Fig. 7c). The fibrolite needles may also be concentrated in folia parallel to the short axis of the nodules or, less often, in cross cutting folia, parallel to the long and short axes of the nodules (Fig. 7c).

Quartz and plagioclase crystals show lenticular or anhedral shapes. Most frequently fibrolite forms folia around the lenticular quartz crystals (Fig. 7a).

In one sample, fibrolite coexists with prismatic sillimanite, but the sillimanite does not show any microstructural evidence of nucleation or replacement by fibrolite (Fig. 7d).

In some nodules, tourmaline is optically zoned and contains plagioclase inclusions. Some tourmaline grains show incipient fibrolitization and
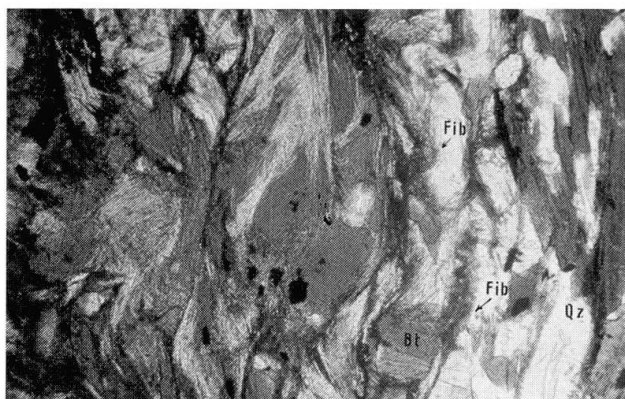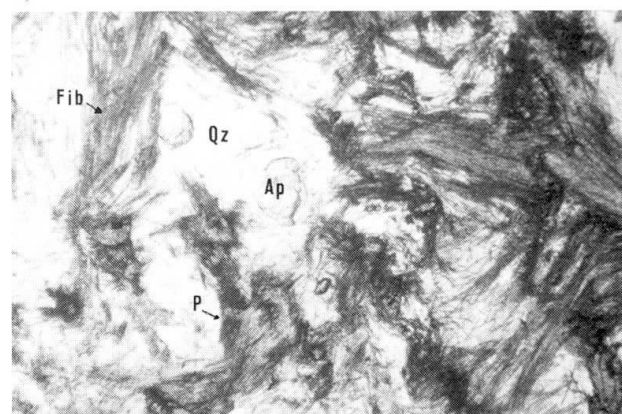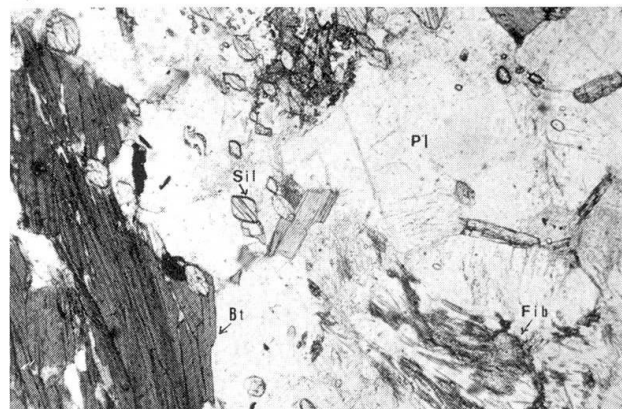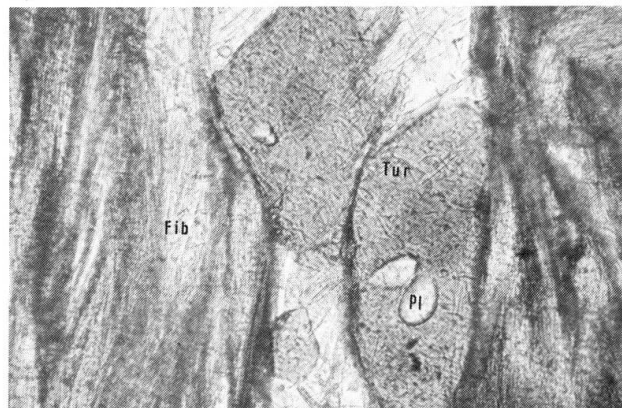
Fig. 7 Photomicrographs of fibrolite nodules: a) Fibrolite growing on and around biotite and quartz. Note the lenticular shape of quartz and the different stage of fibrolitization on the biotite grains. On the right side of the photo at the margin of the nodule, note the unfibrolitized S_2 biotite of melanocratic gneisses. Width of photo corresponds to 2.6 mm. b) Extensively fibrolitized biotite grains. Note the triangular arrangement of fibrolite needles within the biotite basal sections and the orientation of fibrolite needles parallel to the cleavage (001) within the (hk0) biotite sections. Width of photo corresponds to 0.65 mm. c) Fibrolite in single needles, radiating aggregates and pseudomorphic aggregates (p). The latter represent the end product of the biotite fibrolitization. Width of photo 1.3 mm. d) Fibrolite around the prismatic sillimanite in a plagioclase-rich nodule. Width of photo corresponds to 2.6 mm. e) Fibrolitized tourmaline grains enclosing three small plagioclase grains. Width of photo corresponds to 1.3 mm. Mineral abbreviations as in Fig. 1.

their margins appear to be truncated by the formation of fibrolite folia (Fig. 7e).

The textures of the nodules are not consistent with the formation of fibrolite by thermal decomposition of muscovite. The lack of primary muscovite is typical of melanocratic gneisses from NE Sardinia. Muscovite is present in some samples and nodules but it may be easily interpreted as retrograde since it replaced both biotite and fibrolite.

On the contrary the nodules preserved textural evidence that most fibrolite formed from the decomposition of biotite. CHINNER (1961) suggests that the triangular geometrical arrangement of fibrolite in the basal biotite sections matches that of the tetrahedral layer of the biotite structure. In other words the nucleation of fibrolite, that contains the tetrahedrally coordinated chain, was facilitated by the chain-like structure in the tetrahedral layer of the host biotite (KERRICK, 1987). The reaction:

(1)   biotite + H^+ = fibrolite + SiO_2(aq) +
         + (K^+, Mg^{2+}, Fe^{2+}) + H_2O
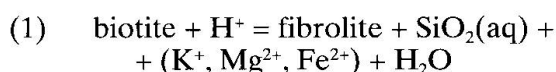
(VERNON, 1979; KERRICK, 1987) could be proposed for the fibrolitization of biotite. This reaction is also consistent with the fact that quartz, biotite and fibrolite formed 95–99% of the nodules. Fibrolite produced by reaction (1) is approximately one-third that of the parent biotite (CHINNER, 1961). Consequently in nodules very rich in fibrolite, it cannot be excluded that some Al and Si was derived from outside the mica or introduced into the rocks with a fluid phase.

According to FOSTER (1990 quoted in KERRICK, 1990) the ferromagnesian components diffusing from the decomposition of biotite within the core of fibrolite nodules could react with the plagioclase of the host rocks to form the biotite-rich rim around the nodules.

In the fibrolite nodules from NE Sardinia there is a close relationship between the presence of the biotite rim and the position of the nodules in mesofolds. In the flank fold zone the nodules often lack of the biotite rim (Figs 5 a, b), while in the hinge fold zone the nodules are surrounded by a thick biotite rim or biotite aureoles. Biotite aureoles are commonly observed around folded fibrolite nodules (Fig. 4). The aureoles are often larger in size than the related nodules.

It is possible that the hinge fold regions may be a preferential sink for the accumulation of ferromagnesian components diffusing from the dissolution of biotite within the core of the nodules and thus an ideal place for the development of the biotite-rich rim.

STRUCTURAL EVIDENCE

On the basis of field and microstructural observations a schematic model for the formation of nodules is depicted in figure 8, starting with country rocks at the end of the S_1 schistosity development and presenting the features observed in the melanocratic gneisses.

The model proposed for the formation of fibrolite nodules involves two distinct processes: the formation of fibrolite in lens-shaped segregations, and the subsequent transformation of the latter in nodules by tectonic deformation.

There are two main data suggesting that most of the fibrolite formed in lens-shaped segregations of variable dimensions: 1) lens-shaped segregations of fibrolite parallel to the S_1 schistosity were actually observed in the field; 2) the reconstruction of the rock fabric prior to the D_2 deformation clearly shows that many adjacent nodules were attached to each other to form lenses. This is evident in figure 4 where four nodules are folded and slightly transposed by D_2 deformation. It clearly appears that before the D_2 deformation the nodules were attached to form a lens of at least 5–7 cm, parallel to the S_1 schistosity.

The close association between veining and fibrolite segregation in space (i.e. occurrence in the same hand specimen) and in time (i.e. between D_1 and D_2 deformations) strongly suggests that the formation of lenses was associated to failures including large fluid filled voids, whose origin could be explained by taking into account the work of OLIVER et al., 1990. According to these authors the strain variation arising as a consequence of the deformation of two rheologically heterogenous rock bodies (i.e. orthogneisses and melanocratic gneisses in the present case) may produce a large amount of failures and a local fluid circulation within and around the boundary. In this light the lens-shaped segregations are considered the result of a metasomatic interaction between the host rocks and an acidic fluid introduced into the rocks during the veining. The source of fluid and fluid producing process at present have not been studied yet. The association of melanocratic gneiss and migmatite appears to be significant in as much as the formation of fibrolite may be tentatively connected with an aqueous solution in some way connected with the episode of migmatization. The preferential occurrence of fibrolite nodules in strong foliated gneisses around the orthogneiss stresses the role played by rock foliation, at this contact, in channelling the fluid flux.

The formation of lens-shaped fibrolitic segregations started after that of the S_1 development
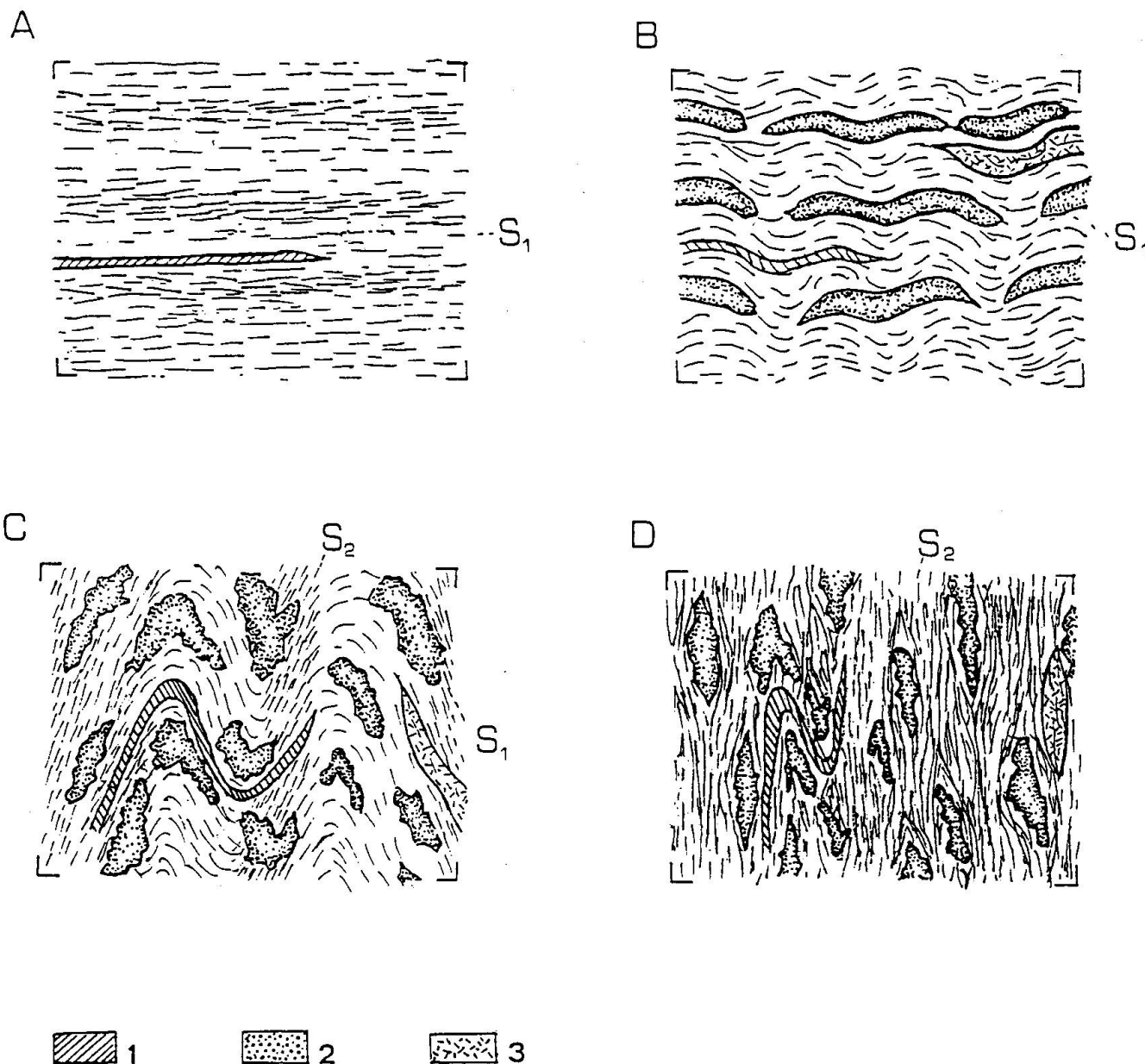
Fig. 8 Sequence of formation events and evolution of nodules in the melanocratic gneisses: a) rocks prior to fibrolite formation; b) crenulation of S_1 and synchronous formation of fibrolite lenses and quartz veins; c) folding of fibrolite lenses, quartz veins and development of tight spaced S_2 schistosity; d) transposition of fibrolite lenses and their transformation into a nodular shape. S = schistosity; 1 = plagioclase-quartz layer; 2 = fibrolite lenses; 3 = quartz veins.

(Fig. 8b). The formation of fibrolite lenses must have been extremely rapid compared to the development of the D_2 deformation. In fact the D_2 phase folded both the S_1 schistosity and the fibrolite lenses.

During the D_2 phase the lenses were first thinned in a series of continuous thick and thin zones (Fig. 8c). They were then progressively thinned and finally cut and transposed by S_2 schistosity. The lenses are extremely reduced in a series of centimetric nodular shapes wrapped in S_2 schistosity. The transposition is also associated with a rotation of adjacent pieces producing a slight asymmetry in the extremity of the nodules (Fig. 8d).

After the D_2 deformation, the fibrolite nodules, whose shape was not significantly modified, underwent late stage muscovitization. The chronological relations between muscovite crystallization and folding indicate that muscovite formed between the D_2 and D_3 folding phases.

Geothermobarometry

The P-T-time path for migmatite from the silli-manite + K-feldspar rocks of NE Sardinia has been described by FRANCESCHELLI et al. (1989). The path involves an early temperature prograde but pressure retrograde stage followed by a stage with falling temperature and pressure. The peak of metamorphism, reached during the early uplift stage, sets at P = 6 kb and T = 700 °C.

In order to evaluate the PT conditions during fibrolite crystallization and late stage muscoviti-zation of the fibrolite nodules, geothermobaro-metric data were collected from the mineral as-semblages of the nodules and of the host rocks. They are summarized in table 2.

The best calibrated geothermometer for the studied rocks is that based on the garnet-biotite exchange reaction (FERRY and SPEAR, 1978). Tak-ing into account the high spessartine content of garnet, the garnet-biotite thermometer was cal-culated using the recent quantitative calibration of GANGULY and SAXENA (1984, 1985). A pressure of 6 Kb estimated by FRANCESCHELLI et al. (1989) for the peak of metamorphism was used for the calculations. The average temperatures for garnet rim- S_2 biotite are: 635 ± 30 °C (GANGULY and SAXENA, 1984) and 620 ± 30 °C (GANGULY and SAXENA, 1985).

According to FRANCESCHELLI et al. (1989) the garnet biotite geothermometer in the rocks of the sillimanite + K-feldspar zone of the Hercynian basement of NE Sardinia does not record the peak metamorphic conditions but only equilibra-tion along the retrograde path.

Recently HOISCH (1989) proposed a geother-mometer based on the exchange of Mg-Tscher-mak's component between muscovite and biotite. According to HOISCH (1989) the application of this geothermometer is restricted to micas that are compositionally similar to those used in the calibration data set. The muscovites and biotites used in the present calculation have all the com-positional requisites suggested by HOISCH (1989).

The muscovite-biotite thermometer, in seven samples, yielded a temperature range of 560–600 °C with an average value of 570 °C. This temperature value is interpreted as the formation temperature of muscovite.

The studied rocks do not record the pressure conditions at the loading stage of the Hercynian orogeny. The only mineralogical evidence of a high pressure stage is given by kyanite relics. However occurrence of pre-D_2 sillimanite sug-gests that the kyanite-sillimanite polymorphic in-version occurred before the peak of metamor-phism.

The phengite barometer (MASSONNE and SCHREYER, 1987) may give useful information on the formation pressure of medium grained mus-covite. The Si content found in medium grained muscovite ranges from 6.05 to 6.18 (a.f.u.). On the basis of the highest Si content of muscovite and assuming a temperature of 570 °C, a pressure of about 4 kb may be estimated. It must be empha-sized that this value provides a minimum pressure estimation if P = P_{H_2O}.

A pressure of 4.0 ± 1.5 kb is also given by the Gt + Bt + Pl+ Ms barometer (HODGES and CROW-LEY, 1985).

In conclusion we cannot set constraints to the P/T formation condition of fibrolite because the melanocratic gneisses do not record the peak metamorphic conditions. However the fibrolite was formed in the stability field of sillimanite at a temperature higher than 620–635 °C, and very probably near the conditions of the metamorphic peak estimated in the adjacent migmatite near T = 700 °C and P = 6 kb.

Geothermobarometry on the muscovitization process affecting the fibrolite nodules and the melanocratic gneisses during the late stage evolu-tion of Hercynian metamorphism can afford very useful P/T information. Geothermobarometric data suggest that muscovite was formed at T = 570 ± 20 °C and P = 4 kb.

The fibrolite in NE Sardinia

At least two types of fibrolite occurrences have been recognized in the sillimanite + K-feldspar zone of the Hercynian basement of NE Sardinia; 1) fibrolite as a major mineral of high grade rocks; 2) fibrolite in the nodules.

The first type of fibrolite (FRANCESCHELLI et al., 1982 b) is widespread in the migmatitic rocks without coexisting prismatic sillimanite. Entry of the K-feldspar + fibrolite pair was observed about 1 km north of the kyanite-sillimanite iso-grad. The second type of fibrolite occurs in nod-ules hosted by melanocratic gneisses in some re-stricted area at the margin of the orthogneisses at Punta Ainu and Monte Longu. This type of fibro-lite coexists with quartz and extensively fibroli-tized biotite.

We conclude that fibrolite in the Hercynian basement of NE Sardinia was formed in two inde-pendent fibrolite forming reactions. The first in-volves the thermal instability of the muscovite plus quartz pair (FRANCESCHELLI et al., 1982 b, 1989). The second involves the instability of biotite in its PT stability field, induced by the activity of hydrogens ions. The latter process

Tab. 2   Summary of P-T metamorphic conditions. T = 620 – 635 °C obtained with the garnet biotite thermometer provides an estimation of a minimum formation temperature of fibrolite. P = 4 kb, T = 570 °C are interpreted as the metamorphic conditions of the formation of muscovite.

Method	Reference	Results
Temperature °C		
* Fe–Mg exchange Grt–Bt	GANGULY and SAXENA (1984)	635 ± 30
* Fe–Mg exchange Grt–Bt	GANGULY and SAXENA (1985)	620 ± 30
* Fe–Mg exchange muscovite-biotite in Al-satured rocks	HOISCH (1989)	570 ± 20
Pressure kb		
* Presence of ky for T = 680 °C	SALJE (1986)	> 6
* Grt–Pl–Bt–Ms	HODGES and CROWLEY (1985)	4.0 ± 1.5
* Phengite barometer for T = 570 °C	MASSONNE and SCHREYER (1987)	4.0

appears to be localized in some restricted areas of the Hercynian basement and mainly in the melanocratic gneisses close to the orthogneisses.

Conclusion

A genetic model including the contemporaneous formation of fibrolite and nodules does not seem appropriate to describe the formation of fibrolite nodules from NE Sardinia.

All the data support the idea that the formation of fibrolite and subsequent origin of the nodules are two distinct processes. Fibrolite was dominantly formed in lens-shaped segregations by decomposition of S_1 biotite produced by a base leaching process. It was formed at the peak of metamorphism, in the PT stability field of sillimanite while the nodules are mainly produced by folding and transposition of fibrolite lenses during the D_2 folding phase.

Acknowledgements

References

CHINNER, G.A. (1961): The origin of sillimanite in Glen Clova, Angus. J. Petrol., 2, 312–323.

ELTER, F.M., FRANCESCHELLI, M., GHEZZO, C., MEMMI, I. and RICCI, C.A. (1986): The Geology of Northern Sardinia. In: Guide-book to the Excursion on the Paleozoic basement of Sardinia – IGCP project n. 5 – Newsletter 1986, special issue, 87–102.

FERRARA, G., RICCI, C.A. and RITA, F. (1978): Isotopic age and tectono-metamorphic history of the metamorphic basement of north eastern Sardinia. Contr. Mineral. Petrol., 68, 99–106.

FERRY, J.M. and SPEAR, F.S. (1978): Experimental calibration of partitioning of Fe and Mg between biotite and garnet. Contr. Mineral. Petrol., 66, 113–117.

FRANCESCHELLI, M., MEMMI, I., PANNUTI, F. and RICCI, C.A. (1989): Diachronic metamorphic equilibria in the Hercynian basement of Northern Sardinia, Italy. In: DALY, J.S.; CLIFT, R.A. and YARDLEY, B.W.H. Eds: "Evolution of metamorphic belts". Geological Society. Special publication N. 43, 371–375.

FRANCESCHELLI, M., MEMMI, I. and RICCI, C.A. (1982a): Ca-distribution between almandine-rich garnet and plagioclase in pelitic and psammitic schists from the metamorphic basement of north-eastern Sardinia. Contr. Mineral. Petrol., 80, 285–295.

FRANCESCHELLI, M., MEMMI, I. and RICCI, C.A. (1982b): Zoneografia metamorfica della Sardegna settentrionale. In Guida alla Geologia del Paleozoico sardo. Guide Geologiche Regionali. Mem. Soc. Geol. It., 137–149.

GANGULY, J. and SAXENA, S.K. (1984): Mixing properties of aluminosilicate garnets: Constraint from natural and experimental data, and application to geothermo-barometry. Am. Mineral., 69, 88–97.

GANGULY, J. and SAXENA, S.K. (1985): Mixing properties of aluminosilicate garnets: Constrains from natural and experimental data, and applications to geothermobarometry: Clarifications. Am. Mineral., 70, 1320.

HENRY, D.J. and GUIDOTTI, C.V. (1985): Tourmaline as a petrogenetic indicator mineral: an example from the staurolite-grade metapelites of NW Maine. Am. Mineral., 70, 1–15.

HOISCH, T.D. (1989): A Muscovite-Biotite geothermometer. Am. Mineral., 74, 565–572.

HODGES, K.V. and CROWLEY, P.D. (1985): Error estimation and empirical geothermobarometry for pelitic systems. Am. Mineral., 70, 702–709.

KERRICK, D.M. (1987): Fibrolite in contact aureoles of Donegal, Ireland. Am. Mineral., 72, 240–254.

KERRICK, D.M. (1990): The Al$_2$SiO$_5$ polymorphs. In: S.W. BAILEY (Editor). Rew. Mineral., Mineral. Soc. Am., 22, 353.

KRETZ, R. (1983): Symbol for rock-forming minerals. Am. Mineral., 68, 277–279.

LOSERT, J. (1968): On the genesis of nodular sillimanitic rocks. 23rd International Geological Congress, 4, 109–122.

MASSONNE, H.J. and SCHREYER, W. (1987): Phengite geobarometry based on the limiting assemblage with K-feldspar, phlogopite and quartz. Contrib. Mineral. Petrol., 96, 212–224.

OLIVER, N.H., VALENTA, R.K., WALL, V.J. (1990): The effect of heterogeneous stress and strain on metamorphic fluid flow, Mary Kathleen, Australia, and a model for a large scale fluid circulation. J. metamorphic Geol., 8, 311–331.

SALJE, E. (1986): Heat capacities and entropies of andalusite and sillimanite: the influence of fibrolitization on the phase diagram of the Al$_2$SiO$_5$ polymorphs. Am. Mineral., 71, 1366–1371.

VERNON, R.H. (1979): Formation of late sillimanite by hydrogen metasomatism (base-leaching) in some high-grade gneiss. Lithos, 12, 143–152.

VERNON, R.H. (1987): Growth and concentration of fibrous sillimanite related to heterogeneous deformation in k-feldspar-sillimanite metapelites. J. Metam. Geol., 5, 51–68.